Bioorganic & Medicinal Chemistry 20 (2012) 6313–6320

Contents lists available at SciVerse ScienceDirect

Bioorganic & Medicinal Chemistry

journal homepage: www.elsevier.com/locate/bmc

Lead optimization studies towards the discovery of novel carbamates as potent AChE inhibitors for the potential treatment of Alzheimer's disease ☆

Kuldeep K. Roy [a], Santoshkumar Tota [b], Tusha Tripathi [a], Subhash Chander [a], Chandishwar Nath [c], Anil K. Saxena [a,*]

[a] Division of Medicinal and Process Chemistry, CSIR Central Drug Research Institute, Lucknow 226 001, India
[b] Division of Pharmacology, CSIR Central Drug Research Institute, Lucknow 226 001, India
[c] Division of Toxicology, CSIR Central Drug Research Institute, Lucknow 226 001, India

ARTICLE INFO

Article history:
Received 3 August 2012
Revised 3 September 2012
Accepted 5 September 2012
Available online 12 September 2012

Keywords:
Alzheimer's disease
AChE
Synthesis
Dementia
Carbamates

ABSTRACT

The optimization of our previous lead compound **1** (AChE IC_{50} = 3.31 μM) through synthesis and pharmacology of a series of novel carbamates is reported. The synthesized compounds were evaluated against mouse brain AChE enzyme using the colorimetric method described by Ellman et al. The three compounds **6a** (IC_{50} = 2.57 μM), **6b** (IC_{50} = 0.70 μM) and **6i** (IC_{50} = 2.56 μM) exhibited potent in vitro AChE inhibitory activities comparable to the drug rivastigmine (IC_{50} = 1.11 μM). Among them, the compound **6b** has been selected as possible optimized lead for further neuropharmacological studies. In addition, the AChE–carbamate Michaelis complexes of these potent compounds including rivastigmine and ganstigmine have been modeled using covalent docking protocol of GOLD and important direct/indirect interactions contributing to stabilization of the AChE–carbamate Michaelis complexes have been investigated.

1. Introduction

Alzheimer's disease (AD) is the most common form of irreversible neurological disorder of elderly patients that affects more than 37 million people worldwide.[1] It is clinically characterized by progressive cognitive impairments or decline defined by a loss of memory and learning ability, together with a reduced ability to perform daily routine activities and a diverse array of neuropsychiatric symptoms such as apathy, verbal and physical agitation, irritability, anxiety, depression, delusions and hallucinations.[2] Characteristic neuropathologic findings include selective neuronal and synaptic losses, extracellular neuritic plaques containing the β-amyloid peptide and neurofibrillary tangles (NFTs) composed of hyperphosphorylated forms of the tau (τ) protein.[3] Existing treatments for mild to moderate AD include the use of acetylcholinesterase (AChE) inhibitors such as tacrine,[4] donepezil,[5] rivastigmine,[6] galanthamine,[7] and the use of *N*-methyl-D-aspartate (NMDA) antagonist memantine.[8] However, these drugs are unable to slow or prevent AD progression, rather can provide symptomatic benefits only and suffer from major drawback of loss of therapeutic potential with time.[9] Thus, increasing daily doses in such circumstances increases the side effects until the pause of the treatment. The major side effects are specifically caused by the peripheral activity of these drugs on cholinesterase enzyme. As the average age is increasing all over the world, and so the AD (66% in the developing countries), there is an urgent need for novel therapeutics, which could act as anti-Alzheimer agents with low or no side effects associated with the known commercial drugs for the treatment of the AD. Specifically, there is a need for new cholinesterase inhibitors with wider therapeutic window, to be useful as potential anti-Alzheimer agents without interacting with peripheral cholinesterase enzymes. Extensive efforts by different researchers in the span of 20 years have led to discovery of a number of potent AChE inhibitors with structural diversity, such as xanthostigmine,[10] physostigmine,[11] phenserine,[12] huperzine-A,[13] *bis*-tacrine,[14] *bis*-huperzin-B,[15] quilostigmine,[16] eptastigmine,[13] Ro-46-5934,[17a] P10358,[17b] CHF2819,[18] memoquin,[19] lipocrine,[19] and huprine-X.[20]

Till date, despite of extensive efforts in the area of neurobiology proposing different hypotheses for AD, the cholinergic hypothesis has been the most productive leading to the four clinically effective drugs (tacrine, donepezil, rivastigmine, galanthamine) for treatment of AD. Interestingly, the development of allosteric agonists and modulators of the muscarinic acetylcholine receptor subtype 1 (mAChR1 or M_1) is being envisaged as a new path in medicinal chemistry for getting new promising AD therapeutics.[21] The ongoing effort to develop more therapeutically efficacious AChE inhibitors is currently driven by the remarkable progress made during the last 20 years in elucidating the structural and functional

☆ The CDRI communication number allotted to this manuscript is 8318.

* Corresponding author. Tel.: +91 (522) 2624273; fax: +91 (522) 2623938.
E-mail address: anilsak@gmail.com (A.K. Saxena).

0968-0896/$ - see front matter © 2012 Elsevier Ltd. All rights reserved.
http://dx.doi.org/10.1016/j.bmc.2012.09.005

properties of the AChE enzyme using X-ray crystallography, computational, and site-direct mutagenesis techniques. Presently, there is an availability of ample information on the functional subsites in the active site gorge of AChE involved in the reactivity of the natural substrate (ACh), synthetic covalent and non-covalent inhibitors. The active site gorge of the AChE can be classified into two sites: (i) the catalytic site (CAS) located at the bottom of the gorge catalyzing the hydrolysis of the substrate, and (ii) the peripheral anionic site (PAS) formed by W279 and Y79 present at the mouth of the gorge, which serves as a relay station for the substrate entry into the active site. The CAS, in turn, comprises anionic subsite, acyl pocket, and oxyanion hole. While the W84 and F330 contribute to the anionic subsite of the CAS, making π–cation interactions with the quaternary group of the substrate, the W233, F288 and F290 form the acyl pocket, which determines the specificity of the substrate ACh. The two residues Y121 and F330 make important contributions to the narrow bottleneck in the midway of the active site gorge.[22] A number of these residues have been experimentally established to be involved in the interactions with the known anticholinesterase agents via both cation–π and π–π stacking interactions.[22]

In the recent past, we have reported the discovery of novel orally potent lead compound **1** (AChE IC_{50} = 3.31 μM) through the state-of-the-art computer-aided drug design techniques including pharmacophore modeling, virtual screening and docking studies.[23] In order to further improve the AChE inhibitory potential, we embarked on further optimization of the identified lead **1** considering the fact that the accommodation of covalent and non-covalent ligands by the AChE is dominated by the hydrophobic interactions.[24,25] It has been evidenced by the X-ray crystallographic studies that the high aromatic content of deeply buried (~20 Å) cylindrical active-site gorge, lined by 14 conserved aromatic amino acid residues, is involved in the strong hydrophobic interactions with AChE inhibitors via both cation–π and π–π stacking interactions. In the present study, we describe the further optimization of the lead compound based on above mentioned hypothesis through the synthesis and pharmacological evaluation of a novel series of 16 carbamates. Among these compounds, the three compounds exhibited promising in vitro AChE inhibitory activities comparable to the existing drug rivastigmine used in the treatment of AD.

2. Results and discussions

2.1. Chemistry

The steps for the synthesis of intermediates and title compounds (**6a–m**, **7a**,**b**) are outlined in Scheme 1, which are essentially same as previously described[23] by us. Briefly, the ring reduction of the 6-methoxyquinoline (**2**) using in situ produced Raney Ni at the room temperature (rt) afforded the first intermediate compound, 6-methoxy-1,2,3,4-tetrahydroquinoline (**3**), which upon reaction with benzyl or 2,4-dichlorobenzyl chloride in the presence of potassium carbonate (K_2CO_3) and potassium iodide (KI) in anhydrous N, *N*-dimethylformamide (DMF) afforded the intermediate compounds **4a** or **4b** respectively. The O-demethylation of the second intermediate (**4a** or **4b**) was achieved using molar solution of boron tribromide (BBr_3) to afford the final hydroxy-intermediates (**5a** and **5b**). The reaction of the final hydroxyl intermediates (**5a** or **5b**) with substituted or unsubstituted alkyl/aryl isocyanates in the nonpolar solvent using the inorganic base afforded title compounds.

2.2. Lead optimization strategies

Considering the fact of the high aromatic content of the active site gorge and the dominating hydrophobic interactions of AChE with its inhibitors, we targeted the site-1 and site-2 of the lead compound **1**[23] (Fig. 1) for site-specific modification/optimization in order to explore the suitable substituent(s) at these two sites to identify novel and more potent AChE inhibitors. In view of this, we replaced the benzyl group attached to the nitrogen of 1,2,3,4-tetrahydroquinoline (site-1) with comparatively more hydrophobic 2,4-dichlorobenzyl group. We attempted major modifications at the site-2 of the lead compound **1**, where both substituted aromatic and long-chain (C_6–C_8) alkyl groups were incorporated in novel derivatives of the lead **1** in view of the important contribution of the hydrophobicity at this site as previously reported by us based on the systematic three-dimensional quantitative structure–activity relationship (3D-QSAR) studies carried out on diverse carbamate-class of AChE inhibitors.[24,25]

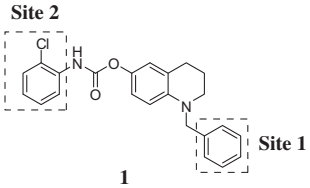

1

AChE IC_{50} = 3.31 μM

Figure 1. The structure and AChE inhibitory activity of the lead compound **1** previously reported from our research laboratory. Sites 1 and 2 are the two sites targeted for the optimization studies presented here.

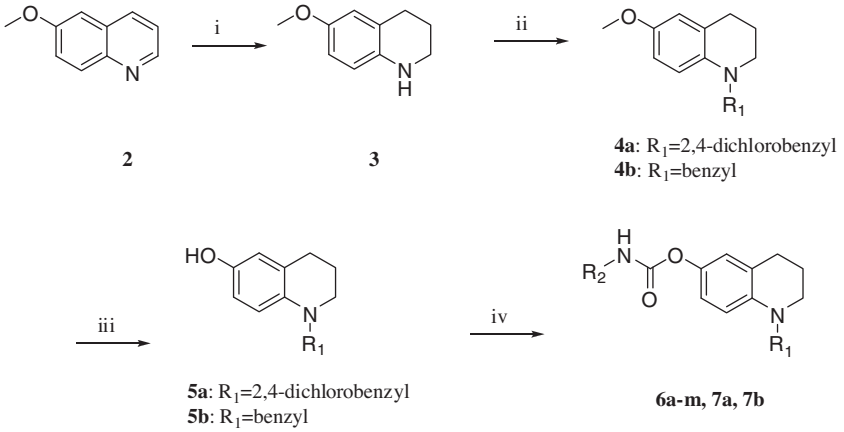

2 **3**

4a: R_1=2,4-dichlorobenzyl
4b: R_1=benzyl

5a: R_1=2,4-dichlorobenzyl
5b: R_1=benzyl

6a-m, 7a, 7b

Scheme 1. Synthesis of carbamates (**6a**–**m**, **7a**,**b**). Reagents and conditions: (i) Nickel−aluminum alloy, ethanol, 10% NaOH in water (w/v), 5−6 h; (ii) R_1-Cl, dry DMF, baked K_2CO_3, KI, rt, 3−5 h; (iii) 1 M BBr_3 in DCM, 3−6 h; (iv) R_2NCO, Et_3N, THF or DCM.

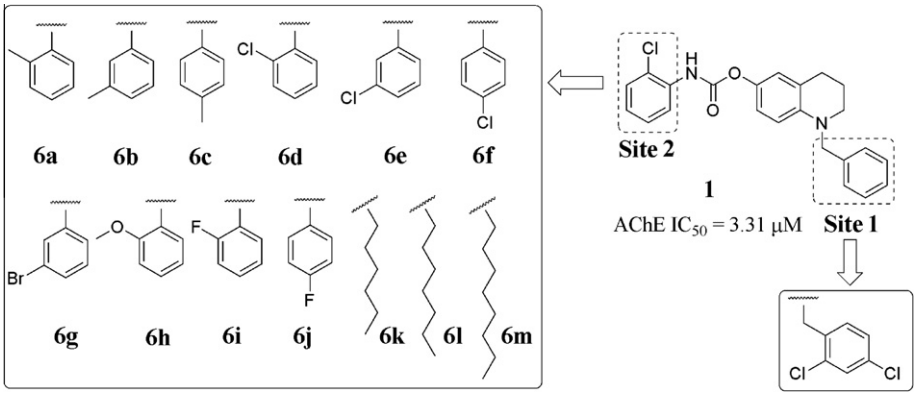

Figure 2. An outline of the synthesized title compounds (**6a**–**m**) based on the site-specific modifications of the lead compound **1**.

Figure 2 outlines the site-specific modifications carried out at the two sites of the lead compound **1** as envisaged.

2.3. Determination of AChE inhibitory activity in vitro

The AChE inhibitory activity of the synthesized novel derivatives (**6a**–**m**, **7a**,**b**) of the lead compound **1** was determined using the Ellman[26] method. The AChE enzyme was purified from red blood cells obtained after the perfusion of the brain of anesthetized adult Swiss albino mice (20–25 g). The kinetic profile of the AChE enzyme activity was studied spectrophotometrically (Shimadzu, USA) and the specific AChE inhibitory activity was calculated on the basis of percent (%) decrease in AChE activity from control values, that is AChE activity without incubation with any standard or test drug. In this assay, tacrine and rivastigmine were used as the two standard AChE inhibitors. Table 1 summarizes the experimentally determined AChE inhibitory activities (IC_{50}, μM) of the compounds (**6a**–**m**, **7a**,**b**) along with rivastigmine and tacrine.

Table 1
Inhibition of AChE by rivastigmine, tacrine and synthesized new compounds (**6a**–**m**, **7a**,**b**)

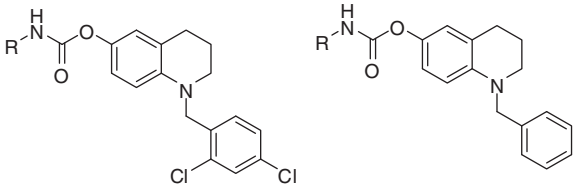

6a-m **7a-b**

Title	R	AChE IC_{50} ± S.E.M. (μM)
1	2-Chlorophenyl	3.31 ± 0.25
6a	2-Methylphenyl	2.57 ± 0.20
6b	3-Methylphenyl	0.70 ± 0.05
6c	4-Methylphenyl	850.60 ± 58.90
6d	2-Chlorophenyl	11.87 ± 2.80
6e	3-Chlorophenyl	210.70 ± 50.10
6f	4-Chlorophenyl	3476.50 ± 68.70
6g	3-Bromophenyl	140 ± 17.10
6h	2-Methoxyphenyl	13.80 ± 0.23
6i	2-Fluorophenyl	2.56 ± 0.28
6j	4-Fluorophenyl	89.37 ± 9.60
6k	Hexyl	14.08 ± 1.70
6l	Heptyl	105.13 ± 22.48
6m	Octyl	>10,000
7a	2-Methylphenyl	14.30 ± 0.23
7b	3-Methylphenyl	60.20 ± 13.40
	Rivastigmine	1.11 ± 0.05
	Tacrine	0.13 ± 0.002

2.4. Structure–activity relationship (SAR) Interpretation

The SAR studies on the synthesized and screened compounds (Table 1) against AChE enzyme suggested that the substitution at the *ortho* (*o*) position of the phenyl ring attached to the carbamyl nitrogen as the most preferred position for the potential inhibition of the AChE enzyme. Among the substituted phenyl groups attached to carbamyl nitrogen, the order of preference was: *ortho* (*o*) > *meta* (*m*) > *para* (*p*) positions for the effective AChE inhibition. These findings corroborated well with our earlier studies[23–25] except the compounds **6b** containing *m*-tolyl at site-2 and 2,4-dichlorobenzyl groups at site-1. This compound **6b** demonstrated the highest AChE inhibitory activity (AChE IC_{50} = 0.70 μM) which was about three fold higher than that of the compound **6a** containing *o*-tolyl group at site-2 (AChE IC_{50} = 2.57 μM), and was comparable to the drug rivastigmine (AChE IC_{50} = 1.11 μM).

Among the compounds with halogen (F, Cl and Br) groups substituted at *ortho*, *meta* and *para* positions of the phenyl ring at site-2, the fluorophenyl derivatives (**6i** and **6j**) exhibited better AChE inhibitory activity than the chlorophenyl (**6d**–**f**) and bromophenyl (**6g**) derivatives. The compound **6i** containing 2-fluorophenyl group at site-2 also exhibited potent AChE inhibitory activity (AChE IC_{50} = 2.56 μM) which was comparable to the compound **6a**. The compound **6h** containing 2-methoxyphenyl group at site-2 exhibited moderate AChE inhibitory activity with AChE IC_{50} of 13.80 μM. Among the compounds with long (C_6–C_8) alkyl groups at the site-2, the compound **6k** containing hexyl chain exhibited moderate AChE inhibition (AChE IC_{50} of 14.08 μM), but was better than the compounds **6l** (IC_{50} = 105.13 μM) and **6m** (IC_{50} >10,000 μM) possessing heptyl and octyl chains respectively at the site-2 (Table 1).

Moreover, it is noteworthy that the introduction of a more hydrophobic group 2,4-dichlorobenzyl at site-1 resulted in the increase in AChE inhibitory activity as the compounds **6a** and **6b** showed better activity than the corresponding compounds (**7a**: 2-methylphenyl; **7b**: 3-methylphenyl) possessing benzyl in place of 2,4-dichlorobenzyl group except the 2-chlorophenyl derivatives (**6d**) which was less active than the corresponding compound **1**.

2.5. Computational modeling of TcAChE–carbamate Michaelis complexes

Among the two X-ray structures of *Tc*AChE (PDB-IDs: 1gqr[27] and 2bag[28]) available in RCSB protein data bank (www.rcsb.org), the bound ligands (rivastigmine and ganstigmine respectively)

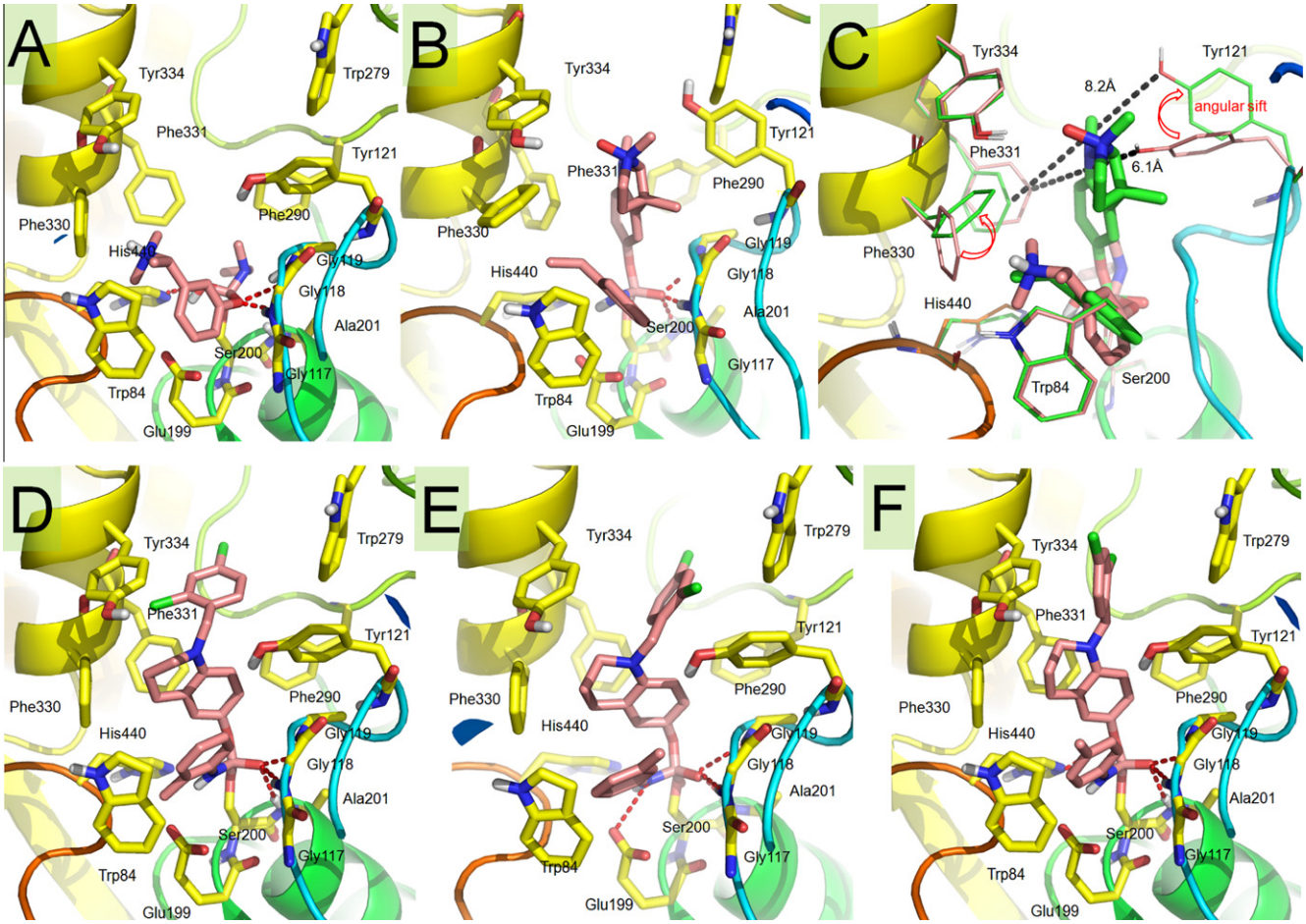

Figure 3. Tetrahedral Michaelis complexes of: (A) *Tc*AChE–rivastigmine. (B) *Tc*AChE–ganstigmine. Ligands are shown in amber-colored stick. (C) The superposed view of the *Tc*AChE–rivastigmine (amber colored) and *Tc*AChE–ganstigmine (green colored) complexes depicting the differences in their orientation and the induced conformations of the active site residues after running 100 ps MDS. (D) *Tc*AChE–compound **6a**; (E) *Tc*AChE–compound **6b**; (F) *Tc*AChE–compound **6c**. The protein is represented as cartoon form.

are present in broken state, with the carbamyl group being covalently bound to the O^{γ} atom of the catalytic site residue Ser200, and the NAP being non-carbamate part of rivastigmine, is located near the anionic subsite characterized by the presence of Trp84 and Phe330 residues,[27] while the geneseroline being non-carbamate part of ganstigmine, is not retained in the catalytic pocket of AChE due to an unknown reason.[28] The 'back door' opening hypothesis has provided an indirect evidence for the release of the leaving group of ganstigmine, physostigmine, and MF268.[29–31] However, its relevance as far as the mechanism of substrate hydrolysis is concerned, remains yet to be established.

Since the rates of formation of the covalent adducts depend primarily on the stabilities of the corresponding AChE–carbamate Michaelis complexes (tetrahedral intermediates), it is imperative to elucidate the specific direct/indirect interactions contributing to stabilization of these complexes. Over the decades, some research groups have reported a number of favorable tetrahedral intermediate of the different covalent (reversible/irreversible) AChE inhibitors in order to explain the rates (kinetics) of the formation of the covalent adducts, and different key interactions playing roles in the stabilization of the AChE–substrate tetrahedral intermediate.[32] It is widely accepted that the carbamylation reaction or covalent adduct formation takes place in two steps: (i) formation of AChE–carbamate Michaelis complexes, (ii) release of the leaving group to result in the carbamylated AChE. A number of kinetic studies[32] on human AChE and BuChE have indicated that the inhibition of AChE by majority of carbamates including rivastigmine is a second-order reaction, while the decarbamylation reaction is a first-order reaction.

In order to gain an insight into the formation of the tetrahedral intermediate and to elucidate the specific direct/indirect interactions contributing to their stabilization, molecular models of *Tc*AChE–carbamate Michaelis complexes for rivastigmine, ganstigmine, and novel discovered compounds (**6a**, **6b**, and **6c**) were generated using the covalent docking protocol available in GOLD docking program, considering the X-ray crystal structure of *Tc*AChE–ganstigmine complex (PDB-ID: 2bag). The small scale (100 ps) molecular dynamics simulations (MDS) using MacroModel[33] suite were performed to relax the initial molecular models to afford stable *Tc*AChE–ligand Michaelis complexes.

Figure 3 depicts the modeled tetrahedral intermediates of the rivastigmine, ganstigmine, and new compounds (**6a**, **6b** and **6c**) with *Tc*AChE. Analyses of these transition states revealed that rivastigmine and ganstigmine, although shared the same binding site, but attained distinct orientation with respect to the active site architecture of *Tc*AChE enzyme. In case of *Tc*AChE–rivastigmine tetrahedral intermediate (Fig. 3A), the positively ionized nitrogen exhibited cation–π interaction with the cation binding subsite-Trp84, and the alkyl groups (methyl and ethyl) attached to the carbamyl nitrogen were occupied the acyl pocket formed by Phe290, Phe292 and Tyr121. In case of *Tc*AChE-ganstigmine Michaelis complex (Fig. 3B), the 2-ethylphenyl group of ganstigmine was projected toward the cation binding subsite-Trp84 exhibiting aromatic π–π interactions and the *o*-ethyl group exhibited

hydrophobic interaction with the two aromatic residues Phe330 and Phe331. The carbonyl oxygen was accommodated in the oxyanion hole through the direct tridentate H-bonds with the amidic NH of the three residues, namely Gly118, Gly119, and Ala201. The particular arrangement of H-bond donors (amidic NH groups of Gly118, Gly119, and Ala201 forming the oxyanion hole) may increase the stability of the TcAChE–carbamate Michaelis complex by favorably accommodating the negatively charged carbonyl oxygen, and thus facilitating the nucleophilic addition by the catalytic residue Ser200, being located in its close proximity, through polarization of the C=O bond of the covalent substrate. Such direct H-bond interactions with the amidic NH groups of the residues forming oxyanion hole are not specifically required for accommodation of non-covalent inhibitors.[32c]

The tricyclic geneseroline group of ganstigmine was extended towards the narrow bottleneck and accommodated in the hydrophobic pocket formed by Tyr121, Phe288, Phe290, and Phe331 (Fig. 3B). However, as aforementioned, this tricyclic group is not retained in the X-ray co-crystal structure of *Tc*AChE–ganstigmine (PDB-ID: 2bag) due to unknown reason. This may be mainly due to its relatively more bulkiness as compared to the leaving group NAP of the rivastigmine. It is noteworthy to note herein that there were apparently some steric perturbations between the tricyclic geneseroline groups and the residues present in the bottleneck region.

In order to explore the conformational landscape of the residues, of the whole AChE–carbamate Michaelis complex, and to confirm the chances of steric perturbations mentioned above, small scale (100 ps) molecular dynamics simulation (MDS) studies were experimented on the *Tc*AChE–carbamate Michaelis complexes. As expected, there was angular shift of the two aromatic residues Phe331 and Tyr121 forming the bottleneck that in turn led into the widening of the gorge opening by about 2 Å as reflected from the superposed view of the *Tc*AChE–rivastigmine and *Tc*AChE–ganstigmine Michaelis complexes (Fig. 3C). Such incidence was not observed in case of *Tc*AChE–rivastigmine after running MDS and the residues in the bottleneck region were quite stable and did not suffer any perturbation(s) due to the small size of the leaving group (NAP) present in the rivastigmine. Our observations are in strong agreement with the reported insights based on the previous molecular modeling and dynamics simulation studies.[29,32,34]

The interaction patterns of the two new potent carbamates (**6a** and **6b**) were very similar to that of the ganstigmine (Fig. 3D and E). Examination of these Michaelis complexes revealed that the *o*-tolyl and *m*-tolyl groups in compounds **6a** and **6b** respectively was located in the cation binding subsite-Trp84, exhibiting hydrophobic interactions with Trp84, Phe330 and Phe331. However, the compound **6c**, which is an structural analogue of the compounds **6a** and **6b**, exhibited steric perturbation (distance $\leqslant$2.5 Å) with the residue Trp84, which was unfavorable towards the stability of the resulting complex and thus, for potential inhibition of the AChE (Fig. 3F). The favorable interaction with this aromatic residue (Trp84) has previously been reported[32] to be highly crucial for the stabilization of Michaelis complex and hence, for carbamylation process of AChE. The unfavorable steric perturbation of *p*-tolyl group of the compound **6c** with Trp84 may be suggested to be one of the potential reasons behind its poor AChE inhibitory activity (IC_{50} = 850.60 μM) compared to its other two structural analogues (**6a** and **6b**). However, unlike ganstigmine, the leaving group 1-(2,4-dichlorobenzyl)-1,2,3,4-tetrahydroquinolin-6-ol, common in these new compounds (**6a–c**) did not suffer from any steric perturbations with the residues forming the bottleneck as assured using small scale MDS (100 ps). This leaving group exhibited hydrophobic interactions with the surrounding residues, namely Trp279, Leu282, Ile287, and Tyr334 (Fig. 3D–F). The chloro groups attached to 2nd and 3rd positions of the phenyl ring are in hydrophobic contacts with the two aliphatic residues Leu282 and Ile287.

3. Conclusion

Considering the evidence from the X-ray crystallographic and computational studies, that hydrophobic interaction plays key role in the accommodation of ligands within the active-site gorge of AChE, we have embarked on the optimization of the previously discovered lead compound **1** (AChE IC_{50} = 3.31 μM). For this, we have synthesized and evaluated a series of novel compounds which has led to the discovery of the three novel promising compounds, **6a** (IC_{50} = 2.57 μM), **6b** (IC_{50} = 0.70 μM) and **6i** (IC_{50} = 2.56 μM) with almost comparable in vitro AChE inhibitory activities as compared to the drug rivastigmine (IC_{50} = 1.11 μM). Among these three compounds, the compound **6b** has been identified as possible optimized lead for further detailed in vivo neuropharmacological studies. Furthermore, the AChE–carbamate Michaelis complexes of these potent compounds including rivastigmine and ganstigmine have been modeled using covalent docking method implemented in GOLD and important structural factors governing the complex stability have been investigated.

4. Experimental section

4.1. Chemistry

General: Reagents were purchased from common commercial suppliers and were used without further purification. Solvents were purified and dried by standard procedures, when necessary. Chromatographic separations of the synthesized intermediates and title compounds were performed on silica gel (Merck: 100–200 mesh). Thin-layer chromatography was used to monitor the reactions. Melting points (uncorrected) were determined with Büchi 510 apparatus. Characterization of the synthesized compounds was accomplished in the sophisticated analytical instrument facility (SAIF) department of CDRI, Lucknow, India. The IR spectroscopy was carried out using Perkin–Elmer 881 spectrophotometer and the values are expressed as ν_{max} cm^{-1}. Mass spectra (MS) were recorded on a Jeol (Japan) SX 102/DA-6000 Mass Spectrometer. ^1H NMR and ^{13}C NMR spectra were recorded on Bruker Spectrospin spectrometer at 300 and 200 MHz respectively. The chemical shifts are reported in δ scale (ppm) and are relative to tetramethyl silane (TMS) as internal standard. The coupling constants *J* are given Hertz and spin multiplicities are expressed s (singlet), d (doublet), t (triplet), dd (double doublet), and m (multiplet).

4.1.1. General procedure for synthesis of title compounds (6a–m, 7a,b)

A mixture of 1-(2,4-dichlorobenzyl)-1,2,3,4-tetrahydroquinolin-6-ol (**5**, 1 mM) and triethylamine (1.2 mM) in dry tetrahydrofuran (THF) was stirred for half an hour under nitrogen atmosphere at rt. To the stirred reaction mixture, desired isocyanate (1.2 mM) was added at once and then the reaction mixture was further stirred for 24–72 h under N_2 atmosphere at the rt. The duration of the reaction was variable depending upon the nature of isocyanate used. The reaction mixture was concentrated under vacuum and then distilled water (15 mL) was added followed by the extraction with ether (3 × 15 mL). The ether layer was dried over sodium sulfate and concentrated under vacuum to afford the crude product, which was finally chromatographed to give the corresponding final product in good yield.

4.1.1.1. 1-(2,4-Dichlorobenzyl)-1,2,3,4-tetrahydroquinolin-6-yl *o*-tolylcarbamate (6a). This compound was synthesized using the general carbamoylation method by taking a solution of 1-(2,4-dichlorobenzyl)-1,2,3,4-tetrahydroquinolin-6-ol (**5**, 1 mM) and triethylamine (1.2 mM) in dry THF, and *o*-tolyl isocyanate (1.2 mM). % Yield: 81%; mp 105 °C, ^1H NMR ($CDCl_3$, 300 MHz). δ ppm 7.92 (br

s, 1H), 7.49 (s, 1H), 7.26–7.24 (d, J = 7.71 Hz, 2H), 7.21–7.19 (d, J = 5.94 Hz, 2H), 7.09–7.04 (t, J = 7.30 Hz, 1H), 6.88–6.87 (d, J = 2.21 Hz, 1H), 6.81–6.77 (m, 1H), 6.71–6.68 (d, J = 8.88 Hz, 1H), 6.27–6.25 (d, J = 8.82 Hz, 1H), 4.47 (s, 2H), 3.42–3.38 (t, J = 5.55 Hz, 2H), 2.89–2.85 (t, J = 6.18 Hz, 2H), 2.33 (s, 3H), 2.11–2.03 (m, 2H). ^{13}C NMR ($CDCl_3$, 200 MHz). δ ppm 155.12, 143.32, 140.19, 135.47, 134.68, 133.88, 132.51, 131.74, 130.26, 129.12, 127.52, 126.67, 125.58, 122.49, 120.45, 119.37, 114.44, 110.59, 59.83, 50.12, 27.34, 22.11, 20.84. FTIR (KBr): cm^{-1} 3405, 2945, 2819, 2366, 1713, 1598, 1441, 1351, 1246, 1157, 972, 771, 692. ESMS: m/z 442 $(M+1)^+$; HRMS calcd for $C_{24}H_{22}Cl_2N_2O_2$ $(M+1)^+$ 441.1058; found 441.1153.

4.1.1.2. 1-(2,4-Dichlorobenzyl)-1,2,3,4-tetrahydroquinolin-6-yl *m*-tolylcarbamate (6b). This compound was synthesized using the general carbamoylation method by taking a solution of 1-(2,4-dichlorobenzyl)-1,2,3,4-tetrahydroquinolin-6-ol (**5**, 1 mM) and triethylamine (1.2 mM) in dry THF, and *m*-tolyl isocyanate (1.2 mM). % Yield: 81%; ^{1}H NMR ($CDCl_3$, 300 MHz). δ ppm 8.17 (br s, 1H), 7.40–7.34 (m, 3H), 7.28–7.23 (m, 1H), 7.16 (s, 1H), 7.02–6.97 (m, 1H), 6.85–6.84 (d, J = 2.35 Hz, 1H), 6.78–6.74 (d, J = 9.98 Hz, 2H), 6.24–6.21 (d, J = 8.78 Hz, 1H), 4.44 (s, 2H), 3.38–3.34 (t, J = 5.535 Hz, 2H), 2.86–2.83 (t, J = 6.105 Hz, 2H), 2.30 (s, 3H), 2.09–2.02 (m, 2H). ^{13}C NMR ($CDCl_3$, 200 MHz). δ ppm 154.82, 143.44, 141.20, 138.72, 136.00, 135.45, 134.81, 133.91, 131.23, 130.12, 128.25, 126.76, 125.30, 124.48, 123.15, 121.56, 120.44, 119.53, 118.49, 110.51, 60.12, 49.99, 27.52, 22.83, 21.24, 20.76. FTIR (Neat): cm^{-1} 3410, 2948, 2823, 2387, 1714, 1598, 1348, 1254, 1157, 975, 771. ESMS: m/z: 442 $(M+1)^+$; HRMS calcd for $C_{24}H_{22}Cl_2N_2O_2$ $(M+1)^+$ 441.1058; found 441.1156.

4.1.1.3. 1-(2,4-Dichlorobenzyl)-1,2,3,4-tetrahydroquinolin-6-yl *p*-tolylcarbamate (6c). This compound was synthesized using the general carbamoylation method by taking a solution of 1-(2,4-dichlorobenzyl)-1,2,3,4-tetrahydroquinolin-6-ol (**5**, 1 mM) and triethylamine (1.2 mM) in dry THF, and *p*-tolyl isocyanate (1.2 mM). % Yield: 78%; mp 130 °C, ^{1}H NMR ($CDCl_3$, 300 MHz). δ ppm 7.40–7.38 (d, J = 6.33 Hz, 1H), 7.31–7.28 (d, J = 8.18 Hz, 1H), 7.26–7.25 (d, J = 4.95 Hz, 2H), 7.22–7.15 (m, 2H), 7.12–7.09 (m, 2H), 6.83–6.82 (d, J = 2.64 Hz, 1H), 6.76–6.69 (m, 1H), 6.23–6.16 (m, 1H), 4.44 (s, 2H), 3.38–3.34 (t, J = 5.565 Hz, 2H), 2.85–2.81 (t, J = 6.375 Hz, 2H), 2.30 (s, 3H), 2.05–1.99 (m, 2H). ^{13}C NMR ($CDCl_3$, 200 MHz). δ ppm 155.96, 143.37, 142.93, 135.07, 134.25, 133.93, 133.52, 133.05, 129.58, 128.62, 128.41, 127.23, 123.09, 122.19, 121.53, 120.72, 120.05, 119.81, 118.81, 111.05, 50.17, 28.14, 22.33, 21.20. FTIR (KBr): cm^{-1} 3403, 2965, 2839, 2366, 1713, 1600, 1496, 1348, 1239, 1157, 998, 762, 686. ESMS: m/z 442 $(M+1)^+$; HRMS calcd for $C_{24}H_{22}Cl_2N_2O_2$ $(M+1)^+$ 441.1058; found 441.1154.

4.1.1.4. 1-(2,4-Dichlorobenzyl)-1,2,3,4-tetrahydroquinolin-6-yl 2-chlorophenylcarbamate (6d). This compound was synthesized using the general carbamoylation method by taking a solution of 1-(2,4-dichlorobenzyl)-1,2,3,4-tetrahydroquinolin-6-ol (**5**, 1 mM) and triethylamine (1.2 mM) in dry THF, and 2-chlorophenyl isocyanate (1.2 mM). % Yield: 81%; mp 222 °C, ^{1}H NMR ($CDCl_3$, 300 MHz). δ ppm 8.17 (br s, 1H), 7.40–7.34 (m, 3H), 7.28–7.23 (m, 2H), 7.16 (s, 1H), 7.02–6.97 (m, 1H), 6.85–6.84 (d, J = 2.28 Hz, 1H), 6.78–6.74 (d, J = 2.61 Hz, 1H), 6.24–6.21 (d, J = 8.82 Hz, 1H), 4.44 (s, 2H), 3.38–3.34 (t, J = 5.535 Hz, 2H), 2.86–2.83 (t, J = 6.105 Hz, 2H), 2.09–2.02 (m, 2H). ^{13}C NMR ($CDCl_3$, CD_3OD 200 MHz). δ ppm 153.14, 140.58, 134.20, 134.00, 133.32, 132.88, 129.19, 128.98, 128.40, 127.57, 127.20, 127.03, 124.07, 123.77, 122.42, 121.84, 119.74, 110.84, 60.19, 53.28, 49.96, 27.93, 22.09. FTIR (KBr): cm^{-1} 3677, 3291, 2928, 2364, 2340, 1713, 1591, 1476, 1386, 1294, 1232, 1197, 1054, 752. ESMS: m/z 461 (M^+); HRMS calcd for $C_{23}H_{19}Cl_3N_2O_2$ (M^+) 461.0512; found 461.0578.

4.1.1.5. 1-(2,4-Dichlorobenzyl)-1,2,3,4-tetrahydroquinolin-6-yl 3-chlorophenylcarbamate (6e). This compound was synthesized using the general carbamoylation method by taking a solution of 1-(2,4-dichlorobenzyl)-1,2,3,4-tetrahydroquinolin-6-ol (**5**, 1 mM) and triethylamine (1.2 mM) in dry THF, and 3-chlorophenyl isocyanate (1.2 mM). % Yield: 80%; mp 125 °C, ^{1}H NMR ($CDCl_3$ + CD_3OD, 300 MHz). δ ppm 7.60 (s, 1H), 7.45–7.36 (m, 3H), 7.33–7.31 (m, 3H), 7.29–7.26 (m, 2H), 7.06–7.02 (m, 1H), 6.89–6.86 (m, 1H), 4.61 (s, 2H), 3.54–3.50 (t, J = 5.610 Hz, 2H), 2.98–2.93 (t, J = 6.375 Hz, 2H), 2.22–2.18 (m, 2H). ^{13}C NMR ($CDCl_3$, CD_3OD, 200 MHz). δ ppm 153.06, 142.61, 140.64, 139.40, 134.20, 133.94, 133.18, 132.71, 129.56, 129.01, 128.30, 126.86, 122.86, 121.78, 119.64, 118.41, 116.44, 110.66, 59.95, 53.11, 49.82, 27.77, 21.97. FTIR (KBr): cm^{-1} 3677, 3287, 2931, 2365, 2334, 1714, 1615, 1593, 1478, 1299, 1231, 1195, 1055, 757. ESMS: m/z: 461 (M^+); HRMS calcd for $C_{23}H_{19}Cl_3N_2O_2$ (M^+) 461.0512; found 461.0573.

4.1.1.6. 1-(2,4-Dichlorobenzyl)-1,2,3,4-tetrahydroquinolin-6-yl 4-chlorophenylcarbamate (6f). This compound was synthesized using the general carbamoylation method by taking a solution of 1-(2,4-dichlorobenzyl)-1,2,3,4-tetrahydroquinolin-6-ol (**5**, 1 mM) and triethylamine (1.2 mM) in dry THF, and 4-chlorophenyl isocyanate (1.2 mM). % Yield: 82%; mp 158 °C, ^{1}H NMR NMR (CD_3OD, 300 MHz). δ ppm 7.89 (br s, 1H), 7.47–7.46 (d, J = 4.62 Hz, 1H), 7.43–7.40 (m, 2H), 7.37 (s, 1H), 7.27–7.24 (m, 2H), 7.18–7.17 (d, J = 1.5 Hz, 2H), 6.83–6.82 (d, J = 2.76 Hz, 1H), 6.25–6.22 (d, J = 8.82 Hz, 1H), 4.47 (s, 2H), 3.42–3.38 (t, J = 5.640 Hz, 2H), 2.87–2.83 (t, J = 6.225 Hz, 2H), 2.09–2.02 (m, 2H). ^{13}C NMR ($CDCl_3$, CD_3OD, 200 MHz). δ ppm 153.21, 142.43, 140.58, 136.76, 134.52, 133.86, 133.04, 132.57, 128.83, 128.27, 127.64, 126.68, 122.72, 121.64, 119.89, 119.50, 110.50, 59.65, 52.91, 49.67, 48.92, 27.60, 21.82. FTIR (KBr): cm^{-1} 3332, 3106, 3033, 2929, 2844, 2367, 1713, 1601, 1542, 1507, 1349, 1220, 1195, 1012, 826, 691, 560. ESMS: m/z 461 (M^+); HRMS calcd for $C_{23}H_{19}Cl_3N_2O_2$ (M^+) 461.0512; found 461.0533.

4.1.1.7. 1-(2,4-Dichlorobenzyl)-1,2,3,4-tetrahydroquinolin-6-yl 3-bromophenylcarbamate (6g). This compound was synthesized using the general carbamoylation method by taking a solution of 1-(2,4-dichlorobenzyl)-1,2,3,4-tetrahydroquinolin-6-ol (**5**, 1 mM) and triethylamine (1.2 mM) in dry THF, and 3-bromophenyl isocyanate (1.2 mM). % Yield: 80%; mp: 132 °C; ^{1}H NMR ($CDCl_3$, 300 MHz). δ ppm 7.59 (s, 1H), 7.44–7.35 (m, 3H), 7.33–7.31 (m, 3H), 7.27–7.24 (d, J = 2.58 Hz, 1H), 7.01–6.98 (m, 1H), 6.85–6.81 (m, 1H), 4.52 (s, 2H), 3.53–3.50 (t, J = 5.613 Hz, 2H), 2.97–2.93 (t, J = 6.372 Hz, 2H), 2.25–2.14 (m, 2H). ^{13}C NMR ($CDCl_3$, 200 MHz). δ ppm 153.16, 142.71, 140.73, 139.49, 134.29, 134.04, 133.28, 132.81, 129.65, 129.11, 128.39, 126.96, 122.96, 121.88, 119.74, 118.51, 116.54, 110.75, 58.98, 53.65, 49.92, 27.87, 22.07. FTIR (KBr) cm^{-1} 3316, 3039, 2936, 2844, 2368, 1712, 1605, 1505, 1359, 1021, 828, 771, 666. ESMS: m/z 505 $(M+1)^+$; HRMS calcd for $C_{23}H_{19}BrCl_2N_2O_2$ $(M+1)^+$ 505.0007; found 505.0023.

4.1.1.8. 1-(2,4-Dichlorobenzyl)-1,2,3,4-tetrahydroquinolin-6-yl 2-methoxyphenylcarbamate (6h). This compound was synthesized using the general carbamoylation method by taking a solution of 1-(2,4-dichlorobenzyl)-1,2,3,4-tetrahydroquinolin-6-ol (**5**, 1 mM) and triethylamine (1.2 mM) in dry THF, and 2-methoxyphenyl isocyanate (1.2 mM). % Yield: 81%; mp 158 °C; ^{1}H NMR ($CDCl_3$, 300 MHz). δ ppm 8.15 (br s, 1H), 7.42–7.34 (m, 3H), 7.27–7.21 (m, 1H), 7.17 (s, 1H), 7.00–6.95 (m, 2H), 6.87–6.75 (m, 2H), 6.22–6.19 (d, J = 8.84 Hz, 1H), 4.44 (s, 2H), 4.32 (s, 3H), 3.38–3.33 (t, J = 5.537 Hz, 2H), 2.86–2.82 (t, J = 6.111 Hz, 2H), 2.07–2.01 (m, 2H). ^{13}C NMR ($CDCl_3$, 200 MHz). δ ppm 153.21, 141.08, 134.32, 134.11, 133.33, 133.00, 129.22, 128.52, 127.64, 127.27, 124.13, 124.03, 122.93, 122.34, 121.88, 120.31, 119.44, 110.64, 60.04, 58.65, 53.35, 49.98, 27.87, 22.04. FTIR (KBr): cm^{-1} 3676, 3290, 2928, 2364, 2340, 1712, 1647, 1591, 1476, 1386,

1294, 1232, 1197, 1054, 752. ESMS: *m/z*: 456 (M^+); HRMS calcd for $C_{24}H_{22}Cl_2N_2O_3$ (M^+) 456.1007; found 456.0995.

4.1.1.9. 1-(2,4-Dichlorobenzyl)-1,2,3,4-tetrahydroquinolin-6-yl 2-fluorophenylcarbamate (6i). This compound was synthesized using the general carbamoylation method by taking a solution of 1-(2,4-dichlorobenzyl)-1,2,3,4-tetrahydroquinolin-6-ol (**5**, 1 mM) and triethylamine (1.2 mM) in dry THF, and 2-fluorophenyl isocyanate (1.2 mM). % Yield: 80%; mp 133 °C, ^{1}H NMR ($CDCl_3$, 300 MHz). δ ppm 8.17 (br s, 1H), 7.40–7.34 (m, 3H), 7.28–7.23 (m, 1H), 7.16 (s, 1H), 7.02–6.97 (m, 2H), 6.85–6.74 (m, 2H), 6.24–6.21 (d, J = 8.83 Hz, 1H), 4.44 (s, 2H), 3.38–3.34 (t, J = 5.535 Hz, 2H), 2.86–2.83 (t, J = 6.105 Hz, 2H), 2.09–2.02 (m, 2H). ^{13}C NMR ($CDCl_3$, 200 MHz). δ ppm 153.21, 142.16, 139.82, 133.44, 133.24, 132.56, 132.12, 128.43, 128.22, 127.64, 126.44, 123.31, 123.00, 122.27, 121.66, 119.51, 118.98, 110.08, 58.67, 52.24, 49.20, 27.17, 21.71. FTIR (KBr): cm^{-1} 3653, 3303, 2826, 2370, 2341, 1715, 1598, 1495, 1456, 1354, 1258, 1202, 1106, 1060, 847, 755, 654. ESMS: *m/z* 445 (M^+); HRMS calcd for $C_{23}H_{19}Cl_2FN_2O_2$ (M^+) 445.0808; found 445.0873.

4.1.1.10. 1-(2,4-Dichlorobenzyl)-1,2,3,4-tetrahydroquinolin-6-yl 4-fluorophenylcarbamate (6j). This compound was synthesized using the general carbamoylation method by taking a solution of 1-(2,4-dichlorobenzyl)-1,2,3,4-tetrahydroquinolin-6-ol (**5**, 1 mM) and triethylamine (1.2 mM) in dry THF, and 4-fluorophenyl isocyanate (1.2 mM). % Yield: 82%; mp 156 °C, ^{1}H NMR ($CDCl_3$, 300 MHz). δ ppm 8.09 (br s, 1H), 7.49–7.44 (d, 1H), 7.41–7.38 (m, 2H), 7.35 (s, 1H), 7.28–7.23 (m, 2H), 7.19–7.17 (d, J = 4.59 Hz, 2H), 6.83–6.81 (d, J = 6.34 Hz, 1H), 6.25–6.22 (d, J = 8.79 Hz, 1H), 4.47 (s, 2H), 3.41–3.37 (t, J = 5.638 Hz, 2H), 2.87–2.82 (t, J = 6.232 Hz, 2H), 2.09–2.02 (m, 2H). ^{13}C NMR ($CDCl_3$, 200 MHz). δ ppm 153.29, 142.51, 140.66, 136.84, 135.19, 133.94, 133.46, 133.12, 132.65, 128.91, 128.35, 127.72, 126.76, 122.80, 121.72, 119.97, 119.58, 110.58, 60.08, 53.56, 49.75, 27.68, 21.90. FTIR (KBr): cm^{-1} 3156, 3082, 2928, 2856, 2365, 1887, 1712, 1552, 1504, 1448, 1407, 1352, 1313, 1226, 969, 691. ESMS: *m/z* 445 (M^+); HRMS calcd for $C_{23}H_{19}Cl_2FN_2O_2$ (M^+) 445.0808; found 445.0874.

4.1.1.11. 1-(2,4-Dichlorobenzyl)-1,2,3,4-tetrahydroquinolin-6-yl n-hexylcarbamate (6k). This compound was synthesized using the general carbamoylation method by taking a solution of 1-(2,4-dichlorobenzyl)-1,2,3,4-tetrahydroquinolin-6-ol (**5**, 1 mM) and triethylamine (1.2 mM) in dry THF, and *n*-hexyl isocyanate (1.2 mM). % Yield: 84%; ^{1}H NMR ($CDCl_3$, 300 MHz). δ ppm 7.40 (s, 1H), 7.26 (s, 1H), 7.16–7.15 (d, J = 1.17 Hz, 2H), 6.78–6.77 (d, J = 2.7 Hz, 1H), 6.70–6.66 (m, 1H), 6.21–6.18 (d, J = 8.82 Hz, 1H), 4.43 (s, 2H), 3.37–3.33 (t, J = 5.625 Hz, 2H), 3.26–3.20 (m, 2H), 2.84–2.80 (t, J = 6.240 Hz, 2H), 2.06–1.98 (m, 2H), 1.72–1.65 (m, 2H), 1.56–1.50 (m, 3H), 0.92–0.86 (m, 6H). ^{13}C NMR ($CDCl_3$, 200 MHz). δ ppm 155.49, 142.57, 141.47, 134.27, 133.39, 132.93, 129.27, 128.60, 127.14, 122.92, 119.97, 110.96, 50.10, 41.21, 31.74, 29.79, 29.16, 28.05, 26.70, 23.97, 22.59, 22.30, 14.04. FTIR (Neat): cm^{-1} 3454, 3025, 2925, 2862, 2350, 1715, 1616, 1509, 1462, 1362, 1222, 1178, 1022, 765, 668, 578. ESMS: *m/z* 435 $(M+1)^+$; HRMS calcd for $C_{23}H_{28}Cl_2N_2O_2$ $(M+1)^+$ 435.1528; found 435.1542.

4.1.1.12. 1-(2,4-Dichlorobenzyl)-1,2,3,4-tetrahydroquinolin-6-yl n-heptylcarbamate (6l). This compound was synthesized using the general carbamoylation method by taking a solution of 1-(2,4-dichlorobenzyl)-1,2,3,4-tetrahydroquinolin-6-ol (**5**, 1 mM) and triethylamine (1.2 mM) in dry THF, and *n*-heptyl isocyanate (1.2 mM). % Yield: 84%; ^{1}H NMR ($CDCl_3$, 300 MHz). δ ppm 7.43 (s, 1H), 7.28 (s, 1H), 7.15–7.14 (d, J = 1.23 Hz, 2H), 6.80–6.79 (d, J = 2.67 Hz, 1H), 6.72–6.68 (m, 1H), 6.23–6.20 (d, J = 8.85 Hz, 1H), 4.48 (s, 2H), 3.35–3.31 (t, J = 5.626 Hz, 2H), 3.28–3.19 (m, 2H), 2.83–2.80 (t, J = 6.236 Hz, 2H), 2.05–1.97 (m, 2H), 1.73–1.61 (m, 2H), 1.56–1.47 (m, 3H), 0.93–0.83 (m, 8H). ^{13}C NMR ($CDCl_3$, 200 MHz). δ ppm 155.46, 142.54, 141.44, 134.25, 133.36, 132.91, 129.24, 128.57, 127.12, 122.89, 122.13, 119.94, 110.93, 50.08, 41.18, 31.71, 29.77, 29.14, 28.03, 26.67, 23.94, 22.56, 22.28, 14.01. FTIR (Neat): cm^{-1} 3450, 3015, 2930, 2859, 2363, 2340, 1713, 1616, 1507, 1462, 1355, 1219, 1173, 1026, 769, 670. ESMS: *m/z* 449 (M^+); HRMS calcd for $C_{24}H_{30}Cl_2N_2O_2$ (M^+) 449.1684; found 449.1712.

4.1.1.13. 1-(2,4-Dichlorobenzyl)-1,2,3,4-tetrahydroquinolin-6-yl n-octylcarbamate (6m). This compound was synthesized using the general carbamoylation method by taking a solution of 1-(2,4-dichlorobenzyl)-1,2,3,4-tetrahydroquinolin-6-ol (**5**, 1 mM) and triethylamine (1.2 mM) in dry THF, and *n*-octyl isocyanate (1.2 mM). % Yield: 83%; ^{1}H NMR ($CDCl_3$, 300 MHz). δ ppm 7.49 (s, 1H), 7.23 (s, 1H), 7.17–7.16 (d, J = 1.16 Hz, 2H), 6.80–6.79 (d, J = 2.52 Hz, 1H), 6.71–6.68 (m, 1H), 6.22–6.19 (d, J = 8.84 Hz, 1H), 4.45 (s, 2H), 3.37–3.32 (t, J = 5.626 Hz, 2H), 3.29–3.21 (m, 2H), 2.85–2.81 (t, J = 6.238 Hz, 2H), 2.02–1.94 (m, 2H), 1.71–1.64 (m, 2H), 1.55–1.48 (m, 3H), 0.91–0.83 (m, 10H). ^{13}C NMR ($CDCl_3$, 200 MHz). δ ppm 155.55, 142.63, 141.53, 134.33, 133.45, 132.99, 129.33, 128.66, 127.20, 122.98, 122.22, 120.03, 111.02, 50.16, 41.27, 31.80, 29.85, 29.22, 28.11, 26.76, 24.83, 24.03, 22.65, 22.36, 14.10. FTIR (Neat): cm^{-1} 3455, 3022, 2931, 2862, 2345, 1712, 1617, 1508, 1463, 1362, 1178, 1022, 771, 669, 585. ESMS: *m/z* 464 $(M+1)^+$; HRMS calcd for $C_{25}H_{32}Cl_2N_2O_2$ (M^+) 463.1841; found 463.1858.

4.1.1.14. 1-Benzyl-1,2,3,4-tetrahydroquinolin-6-yl o-tolylcarbamate (7a). This compound was synthesized using the general carbamoylation method by taking a solution of 1-benzyl-1,2,3,4-tetrahydroquinolin-6-ol (1 mM)[22] and triethylamine (1.2 mM) in dry THF, and *o*-tolyl isocyanate (1.2 mM). % Yield: 76%; mp 132 °C, ^{1}H NMR ($CDCl_3$, 300 MHz). δ ppm 7.49–7.32 (m, 4H), 7.24–7.19 (m, 5H), 7.05–7.01 (m, 2H), 6.80–6.78 (d, J = 2.18 Hz, 1H), 4.45 (s, 2H), 3.42–3.37 (t, J = 5.68 Hz, 2H), 2.87–2.83 (t, J = 6.12 Hz, 2H), 2.38 (s, 3H), 2.08–2.03 (m, 2H). ^{13}C NMR ($CDCl_3$, 200 MHz). δ ppm 153.92, 143.22, 140.19, 135.37, 134.82, 133.48, 132.11, 131.24, 130.56, 129.72, 126.97, 125.38, 122.19, 120.51, 119.37, 118.25, 114.82, 109.92, 60.13, 52.65, 48.98, 27.43, 22.12, 20.78. FTIR (KBr): cm^{-1} 3405, 2951, 2822, 1713, 1598, 1440, 1245, 1155, 775. ESMS: *m/z* 373 $(M+1)^+$; HRMS calcd for $C_{24}H_{24}N_2O_2$ $(M+1)^+$ 373.1432; found 373.1434.

4.1.1.15. 1-Benzyl-1,2,3,4-tetrahydroquinolin-6-yl *m*-tolylcarbamate (7b). This compound was synthesized using the general carbamoylation method by taking a solution of 1-benzyl-1,2,3,4-tetrahydroquinolin-6-ol (1 mM)[22] and triethylamine (1.2 mM) in dry THF, and *m*-tolyl isocyanate (1.2 mM). % Yield: 61%; ^{1}H NMR ($CDCl_3$, 300 MHz). δ ppm 7.68 (s, 1H), 7.28–7.23 (m, 8H), 6.83–6.79 (m, 2H), 6.46 (d, J = 8.62 Hz, 1H), 4.44 (s, 2H), 3.38–3.34 (t, J = 5.535 Hz, 2H), 2.86–2.83 (t, J = 6.11 Hz, 2H), 2.32 (s, 3H), 2.07–2.01 (m, 2H). ^{13}C NMR ($CDCl_3$, 200 MHz). δ ppm 153.82, 143.46, 141.05, 138.75, 136.00, 135.43, 134.28, 133.39, 131.23, 128.24, 126.75, 125.73, 124.41, 123.12, 120.44, 119.53, 118.42, 109.91, 59.96, 52.45, 48.89, 27.27, 22.34, 21.05. FTIR (Neat): cm^{-1} 3405, 2951, 2822, 1711, 1598, 1440, 1245, 1155, 975, 771. ESMS: *m/z*: 373 $(M+1)^+$; HRMS calcd for $C_{24}H_{24}N_2O_2$ $(M+1)^+$ 373.1432; found 373.1443.

4.1.2. Biological methods

4.1.2.1. Preparation of AChE enzyme. The adult Swiss albino mice (20–25 g) were perfused under mild ether anesthesia through heart with ice cooled normal saline (0.9% NaCl) to remove blood-born cholinesterase from the brain. After perfusion the whole brain

was taken out. A 10% (w/v) homogenate of brain was prepared first by homogenizing in an Ultra-Turrax T25 homogenizer at a speed of 9500 rpm thrice giving intervals for few seconds in between the runs, with sodium phosphate buffer (0.03 M, pH 7). The brain homogenate in volume of 500 μl was mixed with 1% Triton X-100 (1% w/v in 0.03 M sodium phosphate buffer, pH 7) and centrifuged at 100,000*g* at 4 °C in a Beckman Ultracentrifuge (LE 80, USA), using a fixed angle rotor (80 ti) for 60 min. Supernatant was collected and stored at 4 °C for acetylcholinesterase estimation.

4.1.2.2. Determination of AChE inhibition (Ellman method). The assay of AChE inhibition was performed according to method described by Ellman et al.[26] using the AChE purified from red blood cells. The kinetic profile of the AChE enzyme activity was studied spectrophotometrically (Shimadzu, USA) at a wavelength of 412 nM at an interval of 15 s. The assay for each sample was run in triplicate and each experiment was performed twice. The test substance (dissolved in ethanol) was incubated with enzyme source in different concentrations (0.1–100 μmol) for 30 min at 37 °C prior to obtaining the kinetic profile of AChE activity. Tacrine and rivastigmine (0.1–100 μM) were used as standard AChE inhibitor (standard control). The specific AChE inhibitory activity was calculated on the basis of % decrease in AChE activity from control values that is, AChE activity without incubation with any standard or test drug. Protein was estimated in the brain samples by modified Lowry's method. Bovine serum albumin (BSA) was used as standard.

4.1.2.3. Statistical analysis. The results are expressed as mean ± S.E.M. Statistical analysis of passive avoidance values were performed by *t*-test. The IC_{50} value was calculated by nonlinear regression method using GraphPad Prism[35] software.

4.1.3. Molecular docking and molecular dynamics simulation (MDS)

Docking studies were performed using the covalent docking protocol implemented in the GOLD program,[36] which uses a genetic algorithm (GA) to explore the conformation/orientation space. For each of the 50 independent GA runs, a maximum number of 1,00,000 GA operations were performed on a set of five groups with a population size of 200 individuals; the other GA parameters not mentioned herein were set to default values. Goldscore was used as the scoring function. For each ligand, the first ranked solution was selected for further analysis. To relax the initial *Tc*AChE–carbamate Michaelis complexes, 500 steps of steepest descent minimization was performed followed by small scale (100 ps) molecular dynamics simulations (MDS) using MacroModel[33] suite to identify stable *Tc*AChE–ligand Michaelis complexes. During MDS, all atoms are kept free, while during covalent docking, all atoms of protein were kept rigid.

Acknowledgments

The authors (K.K.R. and S.T.) are thankful to the Indian Council of Medical Research, New Delhi and Council of Scientific and Industrial Research, New Delhi for the financial assistance in the form of a fellowship, and to Sophisticated Analytical Instrument Facility (SAIF) department of Central Drug Research Institute, Lucknow for the characterization of compounds. The technical assistance of Messrs A. S. Kushwaha, Z. Ali and D. Vishwakarma is also acknowledged.

References and notes

1. Mount, C.; Downton, C. *Nat. Med.* **2006**, *12*, 780.
2. Cummings, J. L.; Doody, R.; Clark, C. *Neurology* **2007**, *69*, 1622.
3. Klafki, H. W.; Staufenbiel, M.; Kornhuber, J.; Wiltfang, J. *Brain* **2006**, *129*, 2840.
4. Qizilbash, N.; Whitehead, A.; Higgins, J.; Wilcock, G.; Schneider, L.; Farlow, M. *J. Am. Med. Assoc.* **1998**, *280*, 1777.
5. Prasher, V. P. *Int. J. Geriatr. Psychiatry* **2004**, *19*, 509.
6. Ballmaier, M.; Casamenti, F.; Scali, C.; Mazzoncini, R.; Zoli, M. *Neuroscience* **2002**, *114*, 91.
7. Van Dam, D.; Abramowski, D.; Staufenbiel, M.; De Deyn, P. P. *Psychopharmacology* **2005**, *180*, 177.
8. Aracava, Y.; Pereira, E. F. R.; Maelicke, A.; Albuquerque, E. X. *J. Pharmacol. Exp. Ther.* **2005**, *312*, 1195.
9. Melnikova, I. *Nat. Rev. Drug Disc.* **2007**, *6*, 341.
10. Rampa, A.; Piazzi, L.; Belluti, F.; Gobbi, S.; Bisi, A.; Bartolini, M.; Andrisano, V.; Cavrini, V.; Cavalli, A.; Recanatini, M.; Valenti, P. *J. Med. Chem.* **2001**, *44*, 3810.
11. Möller, H. J.; Hampel, H.; Hegerl, U.; Schmitt, W.; Walter, K. *Pharmacopsychiatry* **1999**, *32*, 99.
12. Winblad, B.; Giacobini, E.; Frölich, L.; Friedhoff, L. T.; Bruinsma, G.; Becker, R. E.; Greig, N. H. *J. Alzheimers Dis.* **2010**, *22*, 201.
13. Rafii, M. S.; Walsh, S.; Little, J. T.; Behan, K.; Reynolds, B.; Ward, C.; Jin, S.; Thomas, R.; Aisen, P. S. *Neurology* **2011**, *76*, 1389.
14. Pang, Y.-P.; Quiram, P.; Jelacic, T.; Hong, F.; Brimijoin, S. *J. Biol. Chem.* **1996**, *271*, 23646.
15. Feng, S.; Wang, Z.; He, X.; Zheng, S.; Xia, Y.; Jiang, H.; Tang, X.; Bai, D. *J. Med. Chem.* **2005**, *48*, 655.
16. Braida, D.; Sala, M. *CNS Drug Rev.* **2001**, *7*, 369.
17. (a) Borroni, E.; Damsma, G.; Giovacchini, C.; Mutel, V.; Jakob-Rötne, R.; Da Prada, M. A. *Biochem. Soc. Trans.* **1994**, *22*, 755; (b) Smith, C. P.; Bores, G. M.; Petko, W.; Li, M.; Selk, D. E.; Rush, D. K.; Camacho, F.; Winslow, J. T.; Fishkin, R.; Cunningham, D. M.; Brooks, K. M.; Roehr, J.; Hartman, H. B.; Davis, L.; Vargas, H. M. *J. Pharmacol. Exp. Ther.* **1997**, *280*, 710.
18. Trabace, L.; Cassano, T.; Loverre, A.; Steardo, L.; Cuomo, V. *CNS Drug Rev.* **2002**, *8*, 53.
19. Bolognesi, M. L.; Rosini, M.; Andrisano, V.; Bartolini, M.; Minarini, A.; Tumiatti, V.; Melchiorre, C. *Curr. Pharm. Des.* **2009**, *15*, 601.
20. Camps, P.; Cusack, B.; Mallender, W. D.; El Achab, R. E.; Morral, J.; Muñoz-Torrero, D.; Rosenberry, T. L. *Mol. Pharmacol.* **2000**, *57*, 409.
21. Decker, M.; Holzgrabe, U. *Med. Chem. Commun.* **2012**, *3*, 752.
22. Ordentlich, A.; Barak, D.; Kronman, C.; Flashner, Y.; Leitner, M.; Segall, Y.; Ariel, N.; Cohen, S.; Velan, B.; Shafferman, A. *J. Biol. Chem.* **1993**, *268*, 17083.
23. Chaudhaery, S. S.; Roy, K. K.; Shakya, N.; Saxena, G.; Sammi, S. R.; Nazir, A.; Nath, C.; Saxena, A. K. *J. Med. Chem.* **2010**, *53*, 6490.
24. Roy, K. K.; Dixit, A.; Saxena, A. K. *J. Mol. Graph. Modell.* **2008**, *27*, 197.
25. Chaudhaery, S. S.; Roy, K. K.; Saxena, A. K. *J. Chem. Inf. Model.* **2009**, *49*, 1590.
26. Ellman, G. L.; Courtney, K. D.; Andres, V., Jr.; Feather-Stone, R. M. *Biochem. Pharmacol.* **1961**, *7*, 88.
27. Sussman, J. L.; Harel, M.; Frolow, F.; Oefner, C.; Goldman, A.; Toker, L.; Silman, I. *Science* **1991**, *253*, 872.
28. Bartolucci, C.; Siotto, M.; Ghidini, E.; Amari, G.; Bolzoni, P. T.; Racchi, M.; Villetti, G.; Delcanale, M.; Lamba, D. *J. Med. Chem.* **2006**, *49*, 5051.
29. Gilson, M. K.; Straatsma, T. P.; McCammon, J. A.; Ripoll, D. R.; Faerman, C. H.; Axelsen, P. H.; Silman, I.; Sussman, J. L. *Science* **1994**, *263*, 1276.
30. Bartolucci, C.; Perola, E.; Cellai, L.; Brufani, M.; Lamba, D. *Biochemistry* **1999**, *38*, 5714.
31. Shen, T.; Tai, K.; Henchman, R. H.; Mccmmon, J. A. *Acc. Chem. Res.* **2002**, *35*, 332.
32. (a) Groner, E.; Ashani, Y.; Schorer-Apelbaum, D.; Sterling, J.; Herzig, Y.; Weinstock, M. *Mol. Pharmcol.* **2007**, *71*, 1610; (b) Bar-On, P.; Millard, C. B.; Harel, M.; Dvir, H.; Enz, A.; Sussman, J. L.; Silman, I. *Biochemistry* **2002**, *41*, 3555; (c) Ordentlich, A.; Barak, D.; Kronman, C.; Ariel, N.; Segall, Y.; Velan, B.; Shafferman, A. *J. Biol. Chem.* **1998**, *273*, 19509; (d) Barak, D.; Ordentlich, A.; Stein, D.; Yu, Q.-S.; Greig, N. H.; Shafferman, A. *Biochem. J.* **2009**, *417*, 213; (e) Harel, M.; Quinn, D. M.; Nair, H. K.; Silman, I.; Sussman, J. L. *J. Am. Chem. Soc.* **1996**, *118*, 2340; (f) Nair, H. K.; Lee, K.; Quinn, D. M. *J. Am. Chem. Soc.* **1993**, *115*, 9939; (g) Tormos, J. R.; Wiley, K. L.; Wang, Y.; Fournier, D.; Masson, P.; Nachon, F.; Quinn, D. M. *J. Am. Chem. Soc.* **2010**, *132*, 17751.
33. MacroModel, version 9.6, Schrödinger, LLC: New York, 2008.
34. Xu, Y.; Colletier, J. P.; Weik, M.; Jiang, H.; Moult, J.; Silman, I.; Sussman, J. L. *Biophys. J.* **2008**, *95*, 2500.
35. GraphPad Prism, version 5.04 for Windows, GraphPad Software: La Jolla, California, USA.
36. GOLD, version 3.0.1; Cambridge Crystallographic Data Centre: Cambridge, UK.